Inorganic Chemistry

Article

pubs.acs.org/IC

Highly Sensitive and Selective Difunctional Ruthenium(II) Complex-Based Chemosensor for Dihydrogen Phosphate Anion and Ferrous Cation

Ze-Bao Zheng,[†,‡] Zhi-Ming Duan,[†] Ying-Ying Ma,[†] and Ke-Zhi Wang*[,†]

[†]College of Chemistry, Beijing Normal University, and Beijing Key Laboratory of Energy Conversion and Storage Materials, Beijing 100875, P.R. China

[‡]College of Chemistry and Chemical Engineering, Taishan University, Taian 271021, P.R. China

Supporting Information

ABSTRACT: The anion-interaction properties of a Ru(II) complex of $[Ru(bpy)_2(Htppip)](ClO_4)_2 \cdot H_2O \cdot DMF$ (**RuL**) {bpy =2,2′-bipyridine and Htppip =2-(4-(2,6-di(pyridin-2-yl)pyridin-4-yl)phenyl)-1*H*-imidazo[4,5-*f*][1,10]phenanthroline} were thoroughly investigated in CH_3CN and CH_3CN/H_2O (50:1, v/v) solutions by UV−visible absorption, emission, and ^1H NMR spectra. These analyses revealed that **RuL** acts as an efficient "turn on" emission sensor for $H_2PO_4^-$, and a "turn off" sensor for F^- and OAc^-; in addition, **RuL** exhibited slightly disturbed emission spectra in the presence of the other anions studied (Cl^-, Br^-, I^-, NO_3^-, and ClO_4^-). The cation-sensing properties of **RuL** were also studied in both neat CH_3CN and aqueous 4-(2-hydroxyethyl)-1-piperazineethanesulfonic acid buffer (pH = 7.2)/CH_3CN (71/1, v/v) solutions. **RuL** was found to exhibit a colorimetric sensing ability that was highly selective for Fe^{2+}, as evidenced by an obvious color change from pale yellow to light red-purple to the naked eye over the other cations studied (Na^+, Mg^{2+}, Ba^{2+}, Mn^{2+}, Fe^{3+}, Co^{2+}, Ni^{2+}, Cu^{2+}, Zn^{2+}, Cd^{2+}, Hg^{2+}, and Ag^+). To obtain insights into the possible binding modes and the sensing mechanisms, ^1H NMR spectral analysis, luminescence lifetime measurements, and density functional theoretical calculations were also performed.

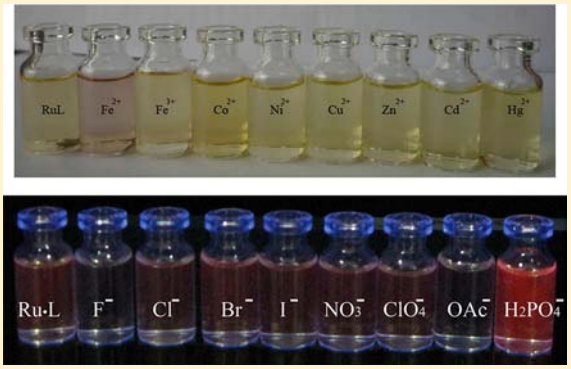

INTRODUCTION

The development of molecular probes that are capable of detecting both cations and anions has attracted considerable attention due to the important roles that cations and the anions play in biological, industrial, and environmental processes.[1] Iron is the most abundant transition-metal ion in humans and other mammals and plays important roles in various biological systems.[2] In contrast, phosphates and their derivatives play important roles in signal transduction and energy storage in biological systems.[3] These facts make it interesting to sensitively and selectively detect Fe^{2+} and $H_2PO_4^-$ ions. Unfortunately, only a few colorimetric anion sensors are able to differentiate effectively between F^-, OAc^-, and $H_2PO_4^-$.[4] A number of organic compounds containing pyrrole, imidazole, urea, or thiourea moieties that are capable of providing an acidic −NH group have been reported to exhibit strong affinity and selectivity toward certain anions.[5] Different types of ligands with N, O, or S donor centers have been reported to act as binding sites for several transition metal cations.[6] However, these organic molecules have small Stokes' shifts and limited photostability. Luminescent transition metal complexes have the obvious advantage of large Stokes' shifts over their purely organic counterparts. However, their great potential as cation and anion sensors has not yet been fully explored.[7] Of the transition metal complexes that have been studied, ruthenium polypyridyl complexes are one of the most investigated chemical systems due to their remarkable chemical stability and intriguing ground- and excited-state photophysical and redox properties. Taking advantage of these favorable properties, optical and electrochemical sensors based on the ruthenium polypyridyl complexes have been rapidly developed for the detection of anions and transition metal cations,[8,9] but the development of highly sensitive and selective multifunctional sensors for both cations and anions still faces a great challenge.[10]

The sensing of cations in aqueous media or even water-organic mixed solvents is a more challenging task than in neat organic solvents; however, this is a key issue for practical applications. We have recently reported that 2-(4-(2,6-di(pyridin-2-yl)pyridin-4-yl)phenyl)-1*H*-imidazo[4,5-*f*][1,10]-phenanthroline (**Htppip**)[1j] acts as fluorimetric sensor for Zn^{2+} and Cd^{2+}, and a colorimetric sensor for Fe^{2+} and F^- anion due to its strong and directed metal-coordinating terpyridine[11] and

Received: July 17, 2012
Published: February 14, 2013

Scheme 1. Synthetic Approach to $[Ru(bpy)_2(Htppip)]^{2+}$ with Numbering Scheme for Proton NMR Signal Assignments

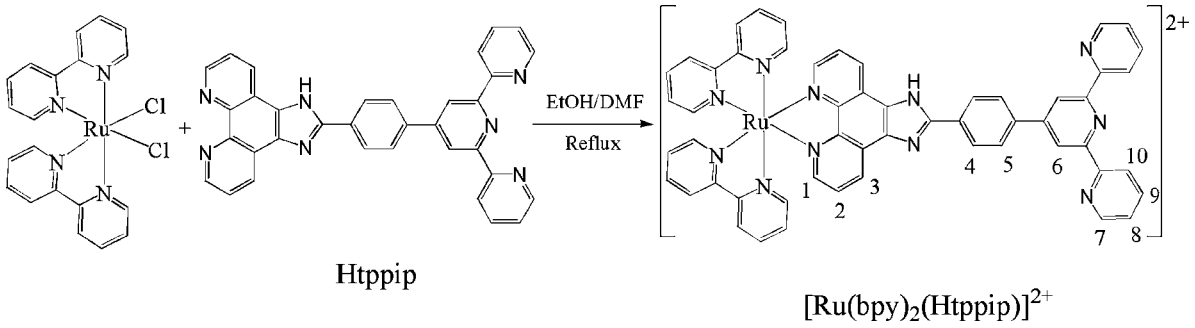

Htppip $[Ru(bpy)_2(Htppip)]^{2+}$

imidazole NH moieties, which act the receptor functional groups for the cations and the anions, respectively. However, the utilization of this sensor in a CH_3CN-H_2O solution with a water content of up to 40% volume ratio is hampered by the poor solubility of **Htppip** and the absence of the magenta color of the **L**/Fe^{2+} complex.[1j] To further improve its water solubility and sensing properties, we have synthesized a Htppip-based Ru(II) complex $[Ru(bpy)_2(Htppip)]^{2+}$ with a phenanthroline moiety coordinated to $Ru^{II}(bpy)_2$ fragments as a first-coordination sphere, and the imidazole NH proton and the uncoordinated terpyridine moiety as the second-coordination sphere for the purpose of sensing and selective recognition of anions and cations, respectively. Interestingly, we found that $[Ru(bpy)_2(Htppip)]^{2+}$ acted as a highly selective and sensitive emission chemosensor for $H_2PO_4^-$ over F^- and OAc^- and a colorimetric sensor for the Fe(II) ion. We report these interesting findings in this manuscript.

EXPERIMENTAL SECTION

Materials. All of the reagents used for synthesis were obtained commercially and were used without further purification. The perchlorate salts of metal cations (Na^+, Mg^{2+}, Ba^{2+}, Mn^{2+}, Fe^{2+}, Fe^{3+}, Co^{2+}, Ni^{2+}, Cu^{2+}, Zn^{2+}, Cd^{2+}, Hg^{2+}, and Ag^+) and the tetrabutylammonium salts of anions (F^-, Cl^-, Br^-, I^-, OAc^-, NO_3^-, ClO_4^-, and $H_2PO_4^-$) were purchased from Aldrich and stored in a vacuum desiccator. *cis*-$[Ru(bpy)_2Cl_2]\cdot 2H_2O$ (bpy = 2,2′-bipyridine) was synthesized according to a protocol described in the literature.[12] **Htppip** was synthesized as previously described[1j] through the condensation of 1,10-phenanthroline-5,6-diamine[13] and 4-(2,6-di(pyridin-2-yl)pyridin-4-yl)benzoic acid.[14] $[Ru(bpy)_2(Htppip)](ClO_4)_2\cdot H_2O\cdot DMF$ (**RuL**) was synthesized as shown in the Supporting Information (SI, see Scheme 1 for the synthetic approach).

Instrumentation. The ^1H NMR spectrum was collected using a Bruker DRX-400 NMR spectrometer with Me_2SO-d_6 as the solvent. The elemental analyses were performed on a Vario EL elemental analyzer. The IR spectrum was recorded on a Nicolet Avatar 360FT-IR spectrometer as KBr disks. The UV−vis absorption spectra were recorded using a GBC Cintra 10e UV−vis spectrophotometer. A high resolution mass spectrum was obtained using an API Q-star pulsar I/oMALDI/Qq-TOF mass spectrometer. The luminescence studies were performed on a Cary Eclipse spectrofluorophotometer (VARIAN) at room temperature. The thermogravimetric and differential thermal analysis (TG-DTA) were conducted using a LCT-1 thermogravimetric/differential thermal analyzer at an temperature elevating rate of 10 °C/min. The luminescence lifetime studies were conducted with a HORIBA Jobin Yvon FluoroMax-4 spectrofluorometer fitted with a time-correlated single photon counting detector and a NanoLED pulsed laser diode excitation source (448 nm).

Optical Sensing Studies. The interaction of **RuL** with various anions and cations was investigated in a CH_3CN or an aqueous 4-(2-hydroxyethyl)-1-piperazineethanesulfonic acid buffer (HEPES, pH = 7.2)/CH_3CN (71/1, v/v) solution. The spectrofluorometric titrations were performed as follows: a stock solution of **RuL** (4.26×10^{-4} M) was prepared in CH_3CN and used in the preparation of titration solution through appropriate dilution of up to 10.0 μM **RuL** in CH_3CN or aqueous 4-(2-hydroxyethyl)-1-piperazineethanesulfonic acid (HEPES) buffer. Microliter aliquots of the anions and cations under investigation were then injected into the sample solution through a rubber septum in the cap. The sample solution was magnetically stirred for 1 min after each addition and, then, was scanned again. This process was repeated until the changes in the UV−vis absorption and luminescence spectra became insignificant. The excitation wavelength λ_{ex} was fixed to 460 nm for the emission measurements.

The binding/equilibrium constants of the Ru(II) complex−anion interactions were evaluated from the absorbance and emission measurements and obtained using the Benesi−Hildebrand eqs 1 and 2, respectively.[15]

$$\frac{1}{A - A_0} = \frac{1}{A_\infty - A_0}\left[\frac{1}{K[G]_i^n} + 1\right] \quad (1)$$

$$\frac{1}{I - I_0} = \frac{1}{I_\infty - I_0}\left[\frac{1}{K[G]_i^n} + 1\right] \quad (2)$$

where A_0 (I_0) and A_∞ (I_∞) are the absorbances (emission intensities) of the free and fully bound forms of **RuL**, respectively, A (I) is the absorbance (emission intensity) of **RuL** in the presence of the cations or anions, n represents the stoichiometry of binding of the cations or anions to **RuL**, K is the association constant of the binding of **RuL** to the cations or the anions, and $[G]_i$ is the concentration of anions or cations added.

Computational Methods. Full geometry optimizations using density functional theory (DFT) with the M06 functional[16] for $[Ru(bpy)_2(Htppip)]^{2+}$ (**1**), $[Ru(bpy)_2(Htppip)]^{2+}\cdot OAc^-$ (**2**), $[Ru(bpy)_2(Htppip)]^{2+}\cdot H_2PO_4^-$ (**3**), and $Fe(II)\cdot\{[Ru(bpy)_2(Htppip)]^{2+}\}_2$ (**4**), respectively, were performed with the Gaussian 09 program.[17] The 6-31G(d) basis set was used for the C, N, O, P, and H elements, and the LanL2DZ pseudopotential[18] was utilized for the ruthenium and ferrous ions.

RESULTS AND DISCUSSION

Synthesis. **RuL** was synthesized through the reaction of stoichiometric amounts of *cis*-$[Ru(bpy)_2Cl_2]$ and **Htppip**[19] in DMF and was characterized by elemental (C, H, and N) analyses, ESI-MS, UV−vis, and ^1H NMR spectroscopic measurements (see the Supporting Information (SI)), which were in agreement with the literature data.[19]

Anion Sensing. *UV−visible Absorption and Emission Spectra.* The UV−vis absorption spectrum of **RuL** in CH_3CN gave rise to a broad metal-to-ligand charge transfer (MLCT) band that was centered at 460 nm ($\varepsilon = 2.82 \times 10^4$ M^{-1} cm^{-1}) and two high-energy intraligand $\pi-\pi^*$ bands at 328 nm ($\varepsilon = 6.85 \times 10^4$ M^{-1} cm^{-1}) and 288 nm ($\varepsilon = 1.54 \times 10^5$ M^{-1} cm^{-1}).

dx.doi.org/10.1021/ic301555r | Inorg. Chem. 2013, 52, 2306−2316

The photoluminescence emission spectrum of **RuL** in CH_3CN showed a broad emission band centered at 608 nm (λ_{ex} = 460 nm). The UV−vis absorption spectra of **RuL** in CH_3CN in the absence and the presence of 10 equiv of the anions (F^-, Cl^-, Br^-, I^-, OAc^-, NO_3^-, ClO_4^-, and $H_2PO_4^-$) are shown in Figure S1 in the SI. Addition of 10 equiv of Cl^-, Br^-, I^-, NO_3^-, and ClO_4^- induced negligible spectral responses in **RuL**, whereas the addition of F^-, OAc^-, and $H_2PO_4^-$ elicited obvious responses in the UV−vis absorption spectra of **RuL**. The results indicate that strong interactions occur between the complex and these three anions. Despite the evident changes in the UV absorption bands, the changes in the visible MLCT absorption band caused by F^-, OAc^-, and $H_2PO_4^-$ were sufficiently weak that the color changes were very marginal to the naked eye (SI Figure S1b), compared with the previously reported ruthenium polypyridyl complex-based sensors for anions, such as $[Ru(bpy)_2(Npnpu)](PF_6)_2$ {Npnpu =1-(6-nitro-[1,10]-phenanthrolin-5-yl)-3-(4-nitrophenyl)-urea}.[20] This finding indicates that **RuL** is not an anion colorimetric sensor. Interestingly, under the illumination of UV light, the luminescence of **RuL** in neat CH_3CN visibly "turned on" to the naked eye upon the addition of $H_2PO_4^-$ (Figure 1a); this

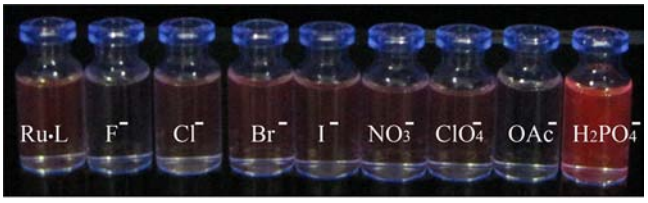

(a)

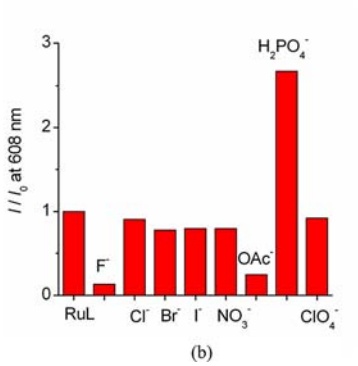

(b)

Figure 1. (a) Photograph taken under UV illumination on **RuL** (1.0×10^{-5} M) in neat CH_3CN in the absence and the presence of 10 equiv of anions. (b) Comparison of the emission intensity ratios of the above-mentioned solutions at 460 nm excitation.

luminescence was invisible upon the addition of F^-, OAc^-, or the other anions studied. In fact, the addition of 10 equiv of $H_2PO_4^-$ resulted in a 3-fold emission enhancement, which is in sharp contrast to considerable quenching of emission intensities of **RuL** by 89% and 83% ("switched off") obtained with the addition of 10 equiv of F^- and OAc^-, respectively, and the slightly altered emissions obtained with the addition of Cl^-, Br^-, I^-, NO_3^-, or ClO_4^- (see Figure 1b). This finding clearly demonstrates the ability of **RuL** to function as a highly selective "turn on" type of luminescence sensor for $H_2PO_4^-$. This type of luminescence $H_2PO_4^-$ sensors based on ruthenium(II) complexes are very scarce because F^-, OAc^-, and $H_2PO_4^-$ usually induced similar spectral changes in Ru(II) complex-based anion sensors (see Table 1),[21] i.e., these three anions typically quench the emission of the Ru(II) complexes. To the best of our knowledge, only several Ru(II) complexes have been reported to exhibit $H_2PO_4^-$-induced emission enhancements, and OAc^-- and F^--induced emission quenching.[9a,22] The luminescence enhancement of **RuL** in the presence of $H_2PO_4^-$ may be caused by the formation of a hydrogen bond between $H_2PO_4^-$ and the imidazolyl N−H of **RuL**; this hydrogen bond results in relatively restricted receptor mobility and an increased rigidity of the **RuL**-$H_2PO_4^-$ complex or the planarity of **RuL**, which accordingly enhances the luminescence of **RuL**.[1i,21e,22] OAc^-- and F^--induced emission quenching of **RuL** is most likely due to the deprotonation of the imidazole moiety of **RuL** by F^- and OAc^-, which is favorable for an intramolecular photoinduced electron transfer from the deprotonated imidazo[4,5-*f*][1,10]phenanthroline moiety to the excited-state Ru center, which results in emission quenching.[23] This type of anion-induced imidazole NH deprotonation is very common because the NH group that is in close proximity to the metal center would become considerably more acidic than that in the free ligand or the group peripheral to the metal center, which would enhance the deprotonation capacity of the complex. To obtain quantitative insight into the binding properties of **RuL** in neat CH_3CN with F^-, OAc^-, and $H_2PO_4^-$, the absorption and emission spectral responses of **RuL** in a CH_3CN solution after successive additions of these three anions were comparatively studied, and the results are shown in Figures 2, 3, and S2 in the SI; these figures also show the OH^- titration results for mechanistic insight. As shown in Figure 2a, incremental additions of OAc^- resulted in evident decreases, evident increases, and slight decreases for the absorption intensities of **RuL** at 328, 368, and 460 nm, respectively; in addition, the addition of OAc^- resulted in the appearance of a new peak at 368 nm, a broad shoulder lingering into long wavelength, and three clear isosbestic points at 351, 430, and 477 nm. As shown in Figure 2b and its inset, the incremental additions of OAc^- to approximately 2 equiv of OAc^- resulted in evident reductions (over 90%) in the emission intensities of **RuL** with a 22-nm redshift in the emission maxima from 608 to 631 nm. As the imidazole NH was deprotonated, the π^* orbital of Htppip ligand is less destabilized than the $Ru^{II}(d\pi)^6$ metal-centered orbital in the excited state complex, resulting in a decrease of the energy gap between $Ru^{II}(d\pi)^6$ and the π^* orbital of Htppip and bathochromic shifts in the emission maxima accordingly.[23] This deprotonation process was also demonstrated by the fact that the UV−vis and emission spectral changes caused by titration with tetrabutylammonium hydroxide (Figures S2a and S2b in the SI) and OAc^- were identical to each other. F^- induced absorption and emission spectral changes (Figures S2c and S2d in the SI) that are similar to those obtained with OAc^-. In contrast, $H_2PO_4^-$ induced two-stage UV−vis absorption spectral changes in **RuL** in CH_3CN (Figure 3a and c), which are different from the one-stage spectral changes observed in the titration of **RuL** with F^- and OAc^-. Successive additions of $H_2PO_4^-$ with a final concentration of 2.0×10^{-5} M (2 equiv) resulted in the first-stage spectral changes in **RuL** (see Figure 3a) that were similar to the spectral changes observed in **RuL** with OAc^- or F^-. However, the marked difference between these changes is the significantly weaker absorption intensity of the band at 368 nm obtained for **RuL** with $H_2PO_4^-$ compared with that obtained with **RuL** with OAc^- and F^-. Upon further additions of $H_2PO_4^-$, the second-stage spectral changes

dx.doi.org/10.1021/ic301555r | Inorg. Chem. 2013, 52, 2306−2316

Table 1. Comparisons of Emission Sensors Based on Representative Ru(II) Complexes

complex	solvent	F^-	OAc^-	$H_2PO_4^-$	ref
$[Ru(bpy)_2(H_2Imdc)](ClO_4)$	acetonitrile	turn on	turn on	turn on	4b
$[Ru(H_2dcbpy)_2(NCS)_2]$	DMSO	turn on	turn on	turn on	8b
$[Ru(Hdcbpy)_2(NCS)_2]Cl_2$	$DMSO/H_2O$				
$[Ru(bpy)_2(Bpsqphen)](ClO_4)_2$	DMSO	turn on	turn on	turn on	21b
	$DMSO/H_2O$				
$[Ru(bpy)_2(Npip)(ClO_4)_2$	DMSO	turn on	turn on	turn on	21d
$[Ru(bpy)_2(H_2iip)](ClO_4)_2$	DMSO	turn off	turn off	turn off	8f
$[Ru(bpy)_2(DMBbimH_2)](PF_6)_2$	CH_3CN	turn off	turn off		21g
$[Ru(bpy)_2(H_2biim)](PF_6)_2$	CH_3CN	turn off	turn off	turn off	21a
$[Ru(H_2pbbzim)(tpy\text{-}HImzphen)](ClO_4)_2$	DMSO	turn off		turn off	21f
$[Ru(bpy)_2(Npnpu)](PF_6)_2$	CH_3CN	turn off	turn off	turn off	20
$[Ru(bpy)_2(H_3Imbzim)](ClO_4)_2$	CH_3CN	turn off	turn off	turn off	21c
$[(bpy)_2Ru(H_2Imbzim)Ru(bpy)_2](ClO_4)_2$	CH_3CN	turn off	turn off	turn off	21c
$[Ru(bpy)_2(Bppnpu)](PF_6)_2$	CH_3CN		turn off	turn on	9a
$[Ru(bpy)_2(Otphendn)](PF_6)_2$	CH_3CN	turn off		turn on	21e
$[Ru(bpy)_2(Htppip)(ClO_4)_2$	CH_3CN	turn off	turn off	turn on	this work
	CH_3CN/H_2O				

[a]Bpsqphen = 6′,7′-bis-(phenylsulfonamido)-quinoxaline-[2′,3′-d]-1,10-phenanthroline-[5,6]; $DMBbimH_2$ = 7,7′-dimethyl-2,2′-bibenzimidazole; H_2biim = 2,2′-biimidazole; Npnpu = 1-(6-nitro-[1,10]phenanthrolin-5-yl)-3-(4-nitrophenyl)-urea); Otphendn = 5,6,8,9,11,12,13,15-octahydro-[1,4,10,13,7,16]tetraoxadiazacyclooctadeca[2,3-*f*][1,10]phenanthroline-3,14(2*H*,4*H*)-dione; $H_2pbbzim$ = 2,6-bis-(benzimidazole-2-yl)pyridine; tpy-HImzphen = 2-(4-[2,2′:6′,2″]terpyridine-4′-yl-phenyl)-1*H*-phenanthro[9,10-*d*]-imidazole; $H_3Imbzim$ = 4,5-bis(benzimidazol-2-yl)imidazole; Bppnpu = 1-(4-[2,2′]Bipyridyl-4-phenyl)-3-(3-nitrophenyl)-urea; Npip = 2′-(*p*-nitrophenyl)-imidazol[4′,5′-*f*]-1,10-phenanthroline[5,6-*f*]; H_2iip = 2-indole-3-yl-imidazole[4,5-*f*][1,10]-phenanthroline; H_2dcbpy = 2,2′- bipyridyl-4,4′-dicarboxylic acid; H_3Imdc = imidazole-4,5-dicarboxylic acid.

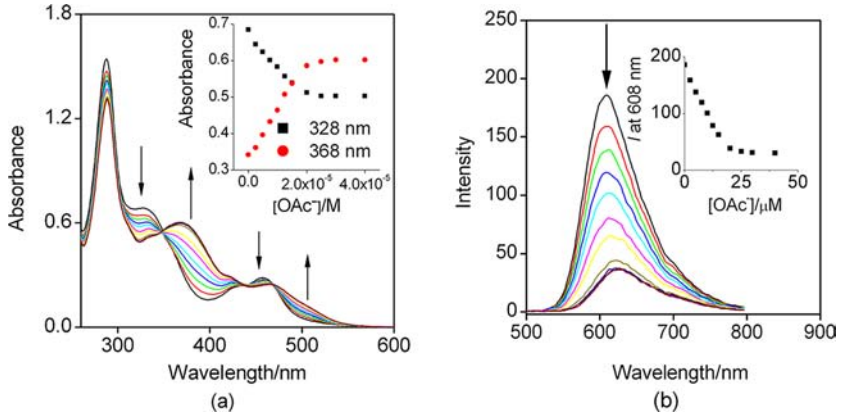

Figure 2. Changes in UV−vis absorption spectra (a) and emission spectra (b) of **RuL** (1.0×10^{-5} M) in CH_3CN upon successive additions of OAc^- (0−4.0 equiv). The insets show changes in absorbance at 328 and 368 nm and in emission intensity (λ_{ex} = 460 nm) versus OAc^- concentrations.

appeared: the absorbances for the $\pi-\pi^*$ transition bands at 290 and 350 nm were significantly decreased (Figure 3c) and were completely different from those (Figure S2a in the SI) observed with the deprotonated **RuL** formed by the addition of Bu_4NOH. $H_2PO_4^-$ induced emission spectral changes (see Figures 3b and d) in **RuL** that were very interesting. Upon the addition of 2.0 equiv of $H_2PO_4^-$, the emission intensities of **RuL** in neat CH_3CN were markedly enhanced by a factor of 2.2 (I/I_0 = 3.2) along with a 7-nm redshift from 608 to 615 nm. Upon further additions of $H_2PO_4^-$, the emission intensities were only slightly decreased (I/I_0 values never decreased by a factor of 2.5) compared with the evident reduction in the emission intensities observed with **RuL** in the presence of Bu_4NOH. These two-stage absorption and emission spectral changes signified the presence of two distinctly different equilibrium processes, and the imidazole NH deprotonation mechanism was thus eliminated. We ascribed the first-stage spectral changes to the hydrogen-bonding interaction of the imidazole NH on **RuL** with $H_2PO_4^-$, and the second one to the formation of a O−H···N hydrogen bond or a proton transfer involving the distal pyridine N of the terpyridine moiety on **RuL** and the OH of $H_2PO_4^-$ as described in the Proton NMR Spectra section.

From the viewpoint of practical applications of anions probes, it is crucial that the probes can be utilized in water-containing media. Therefore, we also investigated the spectral responsing properties of **RuL** in CH_3CN/H_2O (50:1 v/v) in response to anions (see Figures S3−S5 in the SI). Although the addition $H_2PO_4^-$ resulted in one-stage absorption and emission spectral changes (Figures S3a and S3b in the SI) that are different from the two-stage spectral changes observed in neat CH_3CN, these changes resemble the first-stage UV−vis absorption spectral changes observed in neat CH_3CN. It is worth mentioning that the **RuL** exhibited a $H_2PO_4^-$ luminescence sensing capacity in CH_3CN/H_2O (50:1 v/v) with a 3-fold emission enhancement (I/I_0 = 4) and a small 3-nm redshift at titration saturation, which was visualized as a brighter brown-red photoluminescence to the naked eye when

dx.doi.org/10.1021/ic301555r | *Inorg. Chem.* 2013, 52, 2306−2316

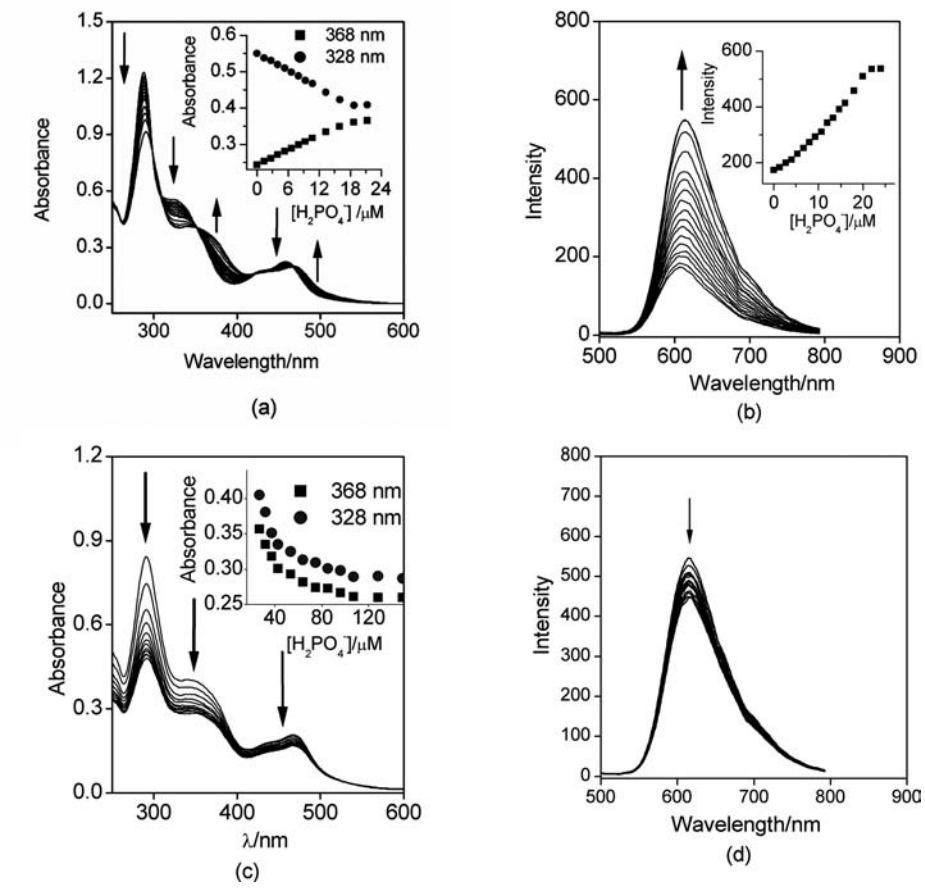

Figure 3. Changes in UV−vis absorption spectra (a and c) and emission spectra (b and d) of 1.0×10^{-5} M **RuL** in CH_3CN upon successively increasing concentrations of $H_2PO_4^-$ from 0 to 2.0×10^{-5} M (a and b) and from 2.0 to 14×10^{-5} M (c and d).

it was excited with a 365 nm UV lamp (Figure S6 in the SI). As more water was added, the detection of $H_2PO_4^-$ became increasingly difficult. For example, 2.0 equiv of $H_2PO_4^-$ were needed to reach saturation in neat CH_3CN compared with the approximately 6.0 equiv $H_2PO_4^-$ that were needed in CH_3CN/H_2O (50:1, v/v) when the concentration of **RuL** was fixed at 1.0×10^{-5} M. In contrast, the emission intensity of **RuL** in CH_3CN/H_2O (50:1, v/v) was effectively quenched by F^- or OAc^- (Figures S4b and S4d in the SI), as observed in neat CH_3CN. The other anions did not significantly affect the absorption and luminescence spectra of **RuL** in the aqueous CH_3CN solution (Figure S5 in the SI). Thus, $H_2PO_4^-$ in water can still be qualitatively detected with the naked eye by dripping one drop of the real water sample containing $H_2PO_4^-$ into the CH_3CN solution containing **RuL**. The stoichiometries between **RuL** and F^-, OAc^-, and $H_2PO_4^-$ were found to be 1:1, 1:1, and 1:2, respectively, by emission Job plots (Figure S7 in the SI). Using eqs 1 and 2, the values of the binding/equilibrium constant K for the **RuL**−anion interactions were evaluated and are shown in Table 2. It is noted that the K values for **RuL** with F^- and OAc^- (1:1) are of the same order of magnitude as those $\{(1.24-3.07) \times 10^4\ M^{-1}\}$ previously reported for $[Ru(bpy)_2(H_2iip)]^{2+}$ {H_2iip = 2-indole-3-yl-imidazole[4,5-*f*][1,10]-phenanthroline} with OAc^- and F^-.[8f] Moreover, the binding constant of **RuL**−$H_2PO_4^-$ in the CH_3CN-H_2O solution is much less than that in the neat CH_3CN solution, which further confirms that the detection of $H_2PO_4^-$ is more difficult in the CH_3CN-H_2O solution than in neat CH_3CN.

Table 2. Equilibrium/Binding Constants[a] (K/M^{-n}) for RuL Toward Various Anions in CH_3CN or CH_3CN/H_2O at 298 K

anions	solvent	stoichiometry 1:*n*	*K* from absorption spectra	*K* from emission spectra
F^-	CH_3CN	1:1	3.53×10^4	3.33×10^4
OAc^-	CH_3CN	1:1	3.27×10^4	3.72×10^4
$H_2PO_4^-$	CH_3CN	1:2	1.02×10^{10}	7.62×10^9
F^-	CH_3CN/H_2O	1:1	4.81×10^4	3.57×10^4
OAc^-	CH_3CN/H_2O	1:1	5.58×10^4	5.13×10^4
$H_2PO_4^-$	CH_3CN/H_2O	1:2	1.18×10^9	1.00×10^9

[a]Estimated errors were <15%.

Proton NMR Spectra. The ^1H NMR spectra of **RuL** in $(CD_3)_2SO$ in the absence and presence of OAc^- and $H_2PO_4^-$ are shown in Figures 4 and 5, respectively. The spectral assignments of the complex were made using the $\{^1H-^1H\}$ COSY spectrum (Figure S8 in the SI) and relative areas of the peaks and by taking into consideration the usual ranges of the J values for Htppip and 2,2′-bipyridine.[4b] The proton numbering scheme used to assign the observed resonances is shown in Scheme 1. To shed light on the nature of the interactions between **RuL** and the anions, ^1H NMR spectral changes obtained upon the addition of OAc^- and $H_2PO_4^-$ as tetrabutylammonium salts to the DMSO-d_6 solution of **RuL** (1×10^{-2} M) were selectively investigated. As shown in Figure

dx.doi.org/10.1021/ic301555r | *Inorg. Chem.* 2013, 52, 2306−2316

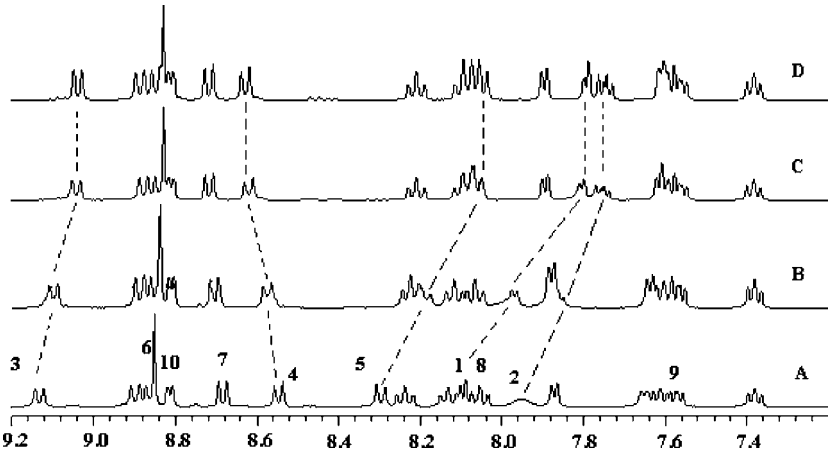

Figure 4. Partial ^{1}H NMR (400 MHz) spectra of **RuL** (1.0×10^{-2} M) in DMSO-d_6 in the absence (A) and the presence of 0.6 (B), 2.0 (C), and 10.0 (D) equiv of $[Bu_4N]^+OAc^-$ (proton labeling shown in Scheme 1).

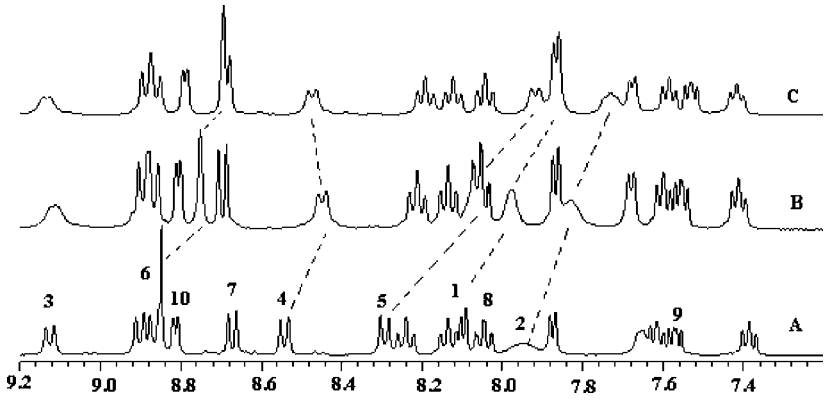

Figure 5. Partial ^{1}H NMR (400 MHz) spectra of **RuL** (1.0×10^{-2} M) in DMSO-d_6 in the absence (A) and the presence of 0.6 (B) and 2.0 (C) equiv of $[Bu_4N]^+H_2PO_4^-$ (proton labeling shown in Scheme 1).

4, although the signal of the N−H proton in Htppip was unobserved in the present case, the chemical shifts of the C−H protons in Htppip were very sensitive to the additions of the anions. However, the proton signals on the bpy ligands were significantly less affected. Upon the addition of 10 equiv of OAc^- into **RuL** in DMSO-d_6, the H_1, H_2, H_3, and H_5 peaks were shifted upfield by $\Delta\delta$ = −0.27, −0.22, −0.10, and −0.25 ppm, respectively. These shifts are attributed to the deprotonation of the imidazole NH moiety by OAc^-,[24] which increased the electron density on the imidazo[4,5-*f*]-1,10-phenanthroline moiety on **RuL**. The downfield shift of the H^4 that was observed was attributed to the formation of a C−H···O hydrogen bond with OAc^-. Using pK_{a2} = 4.75[25a] for HOAc and pK_a = 8.09 for the imidazole NH of **RuL** in 1:100 CH_3CN/Britton−Robinson (BR) buffer (v/v), the matching acidity ΔpK_a {ΔpK_a = pK_{a2} (HOAc) − pK_a (proton donor)} was calculated to be 3.34. This value supports the occurrence of the proton transfer reactions from the imidazole NH on **RuL** to OAc^- compared with the reported matching acidity ΔpK_a value of 2.45 in aqueous solution, which supports a proton transfer reaction in the interaction of $[Ru(bpy)_2(TMBbimH_2)]^{2+}$ ($TMBbimH_2$ = 5,6,5′,6′-tetramethyl-2,2′-bibenzimidazole) with OAc^- in a CH_3CN solution.[25b] As shown in Figure 5, the additions of the $H_2PO_4^-$ to the solution of **RuL** resulted in obvious upfield shifts of $\Delta\delta$ = −0.38, −0.27, −0.06, and −0.23 ppm, respectively, for the H_1, H_2, H_4 and H_5 signals, and a downfield shift and broadening for the H_3 signal. These NMR spectral changes were assigned to a strong double hydrogen-bonding interaction of $H_2PO_4^-$ with the imidazole NH and the H_3 of **RuL**, which increased the electron density on the phenyl-imidazo[4,5-*f*]-1,10-phenanthroline moiety of **RuL** and reduced the electron density of H_3. The stronger deprotonation ability of OAc^- compared with $H_2PO_4^-$ can be understood by the stronger basicity of the former than the latter (pK_a = 4.75 for HOAc compared with pK_{a1} = 2.12 for H_3PO_4)[25a] in an aqueous solution and the fact that OAc^- has a capacity to form complementary linear "Y-type" hydrogen bonds with a receptor.[25c] The AcO^- triangle that has an O−C−O angle of 120° may better simultaneously bind to two receptors (e.g., NH and H_4 in our case) than tetrahedral $H_2PO_4^-$ because $H_2PO_4^-$ has an O−P−O angle of 108°, which implies that the distance between the oxygen atoms of $H_2PO_4^-$ is shorter than that of AcO^- and is therefore unfavorable for the bridging binding to the two receptors. Interestingly, the additions of more $H_2PO_4^-$ (2.0 equiv) caused an obvious upfield shift from 8.85 to 8.69 ppm in the H_6 signal with a slight downfield shift in the H_4 signal. The upfield shift of the H_6 signal was ascribed to the breakage of a C−H_6···N (distal pyridine N of terpyridine) type of intramolecular hydrogen bonding by the formation of a O−H···N hydrogen bond or a proton transfer involving the distal pyridine N of terpyridine and the OH of $H_2PO_4^-$. The slight downfield shift in the H_4 signal may be caused by the partial protonation of imidazole N. The addition of more than 2 equiv of $H_2PO_4^-$ resulted in the appearance of precipitation, which

dx.doi.org/10.1021/ic301555r | *Inorg. Chem.* 2013, 52, 2306−2316

prevented further NMR studies. In 1:100 (v/v) CH_3CN/BR buffer, the values of the acid ionization constants (pK_a) of the conjugate acids of the terpyridine and imidazole N moieties of **RuL** were determined by UV−vis absorption spectrophotometric pH titration to be 3.66 and 1.13, respectively; these values are in agreement with the previously reported pK_a values of 3.16 and 4.60 for two successive protonations of the distal pyridine of 2,2′:6,2″-terpyridine in CH_3OH-H_2O (w/w,16.5:83.5)[25d] and of 2.17 for $[Ru(bpy)_2(Hpip)]Cl_2$ {Hpip =2-phenyl-1*H*-imidazo[4,5-*f*][1,10]phenanthroline},[25c] respectively. Thus, $H_2PO_4^-$ would prefer to interact with the distal pyridine N rather than with the imidazole N of **RuL**. Using a $pK_{a2} = 7.21$[25a] for H_3PO_4, the matching acidity ΔpK_a {ΔpK_a = pK_{a2} (H_3PO_4) − pK_a (proton acceptor)} was calculated to be 4.55 for the proton transfer reactions from $H_2PO_4^-$ to the distal pyridine N of the terpyridine moiety on **RuL**; this value is only 2 pK_a units greater than a previously reported ΔpK_a value of 2.45 in an aqueous solution for the proton transfer reaction in a CH_3CN solution for the interaction of $[Ru(bpy)_2(TMBbimH_2)]^{2+}$ with OAc^-.[25b] Thus, we conclude that the occurrence of a proton transfer reaction from $H_2PO_4^-$ to the distal pyridine N of terpyridine on **RuL** could not be completely eliminated.

Lifetime-Based Signaling. The interaction of **RuL** with OAc^- and $H_2PO_4^-$ was also investigated using the time-resolved luminescence technique. The time-resolved luminescent decay profiles of **RuL** as a function of the OAc^- and $H_2PO_4^-$ concentrations are shown in Figure 6a and b,

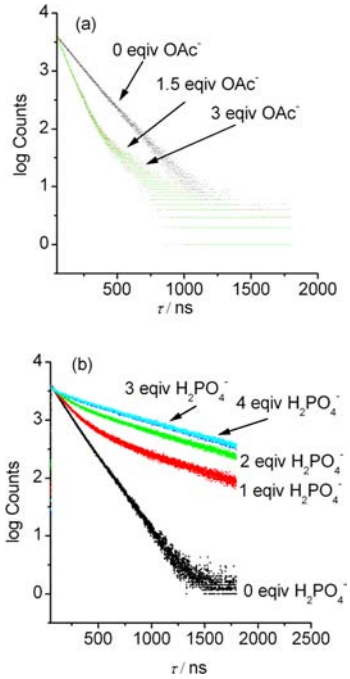

Figure 6. Time-resolved luminescence decay profiles of **RuL** in acetonitrile in the presence of 0, 1.5, and 3.0 equiv of OAc^- (a) and 0, 1.0, 2.0, 3.0, and 4.0 equiv of $H_2PO_4^-$ (b).

respectively. The free **RuL** in acetonitrile at room temperature exhibited a single exponential luminescence decay with a lifetime of 153.2 ± 0.2 ns. In the presence of 1.5 and 3.0 equiv of OAc^-, the luminescent decays were also fitted to the single exponential decays with lifetimes of 77.0 ± 0.1 and 76.1 ± 0.1 ns, respectively, which suggests the formation of the short-lived, imidazole NH deprotonated **RuL**. In the presence of 1.0, 2.0, 3.0, and 4.0 equiv of $H_2PO_4^-$, the decays in luminescence intensities were still fitted to the single exponential model with elongated lifetimes of 212.4 ± 0.6, 385.9 ± 1.6, 610.6 ± 3.2, and 624.3 ± 3.2 ns, respectively; these results are in sharp contrast to the shortening in the luminescence lifetime observed with **RuL** in the presence of OAc^-. These observations in the luminescence lifetimes are in full agreement with the steady-state luminescence measurements and make the Ru(II) complex a selective lifetime-based sensor for $H_2PO_4^-$.

Cation Sensing. *UV−visible Absorption and Emission Spectral Characteristics.* The chemosensing behavior of **RuL** for a variety of metal cations (Na^+, Mg^{2+}, Ba^{2+}, Mn^{2+}, Fe^{2+}, Fe^{3+}, Co^{2+}, Ni^{2+}, Cu^{2+}, Zn^{2+}, Cd^{2+}, Hg^{2+}, and Ag^+) was comparatively investigated in a CH_3CN−pH 7.2 HEPES buffer aqueous solution (1/71 v/v) and in neat CH_3CN. As shown in Figure 7a, the addition of 1 equiv of Fe^{2+} into the Ru complex in the

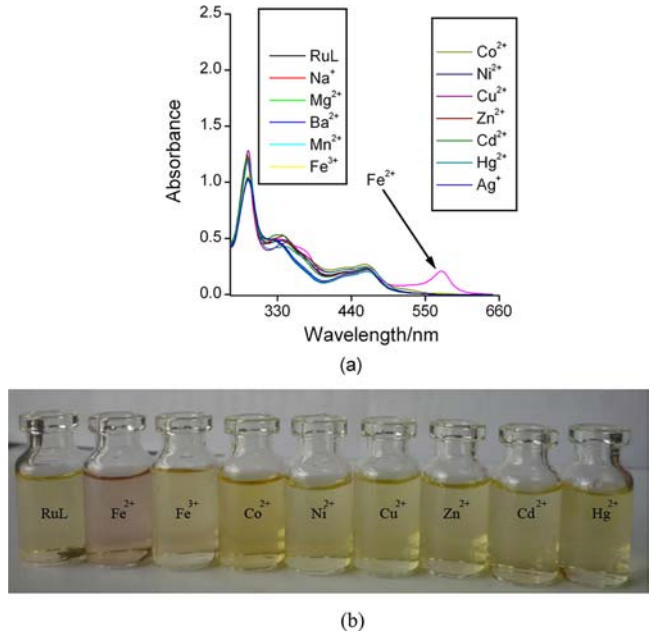

Figure 7. Changes in UV−vis absorption spectra (a) of **RuL** (1.0×10^{-5} M) in aqueous HEPES buffer/CH_3CN (71/1, v/v) solution upon additions of different cations as perchlorate salts (1.0×10^{-5} M) and photographs (b) taken under daylight for the above-mentioned solutions.

CH_3CN aqueous solution produced a strong new band centered at 575 nm, which is in sharp contrast to the very weak absorption for **RuL** in the presence of 1 equiv of Fe^{3+}. Moreover, no visible absorption for **RuL** in the presence of 1 equiv of the other metal ions was observed; therefore, the ferrous cation could be visually distinguished from the other cations studied, as shown in Figure 7b. As shown in Figure 8a, the successive additions of Fe^{2+} (from 0 to 6.0×10^{-6} M, which is equivalent to 0.6 equiv) into the Ru complex in the CH_3CN aqueous solution resulted in obvious intensity decreases in the band at 318 nm, a 5-nm redshift, and the appearance of one new band centered at 575 nm ($\varepsilon = 2.89 \times 10^4$ M^{-1} cm^{-1}); these changes were companied by a solution color change from pale yellow to light red-purple that was vivid to the naked eye due to the coordination of Fe^{2+} to the uncoordinated terpyridine moiety of **RuL**.[11] The absorbances at 575 nm increased linearly with $[Fe^{2+}]$ until $[Fe^{2+}]/[\mathbf{RuL}] = 0.5$. The

dx.doi.org/10.1021/ic301555r | *Inorg. Chem.* 2013, 52, 2306−2316

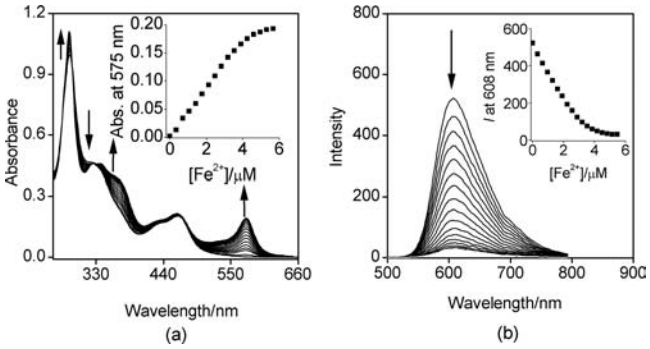

Figure 8. Changes in UV−vis absorption (a) and photoluminescence (b) spectra of **RuL** (1.0×10^{-5} M) in aqueous HEPES buffer/CH_3CN (71/1, v/v) solution upon additions of $Fe(ClO_4)_2$ (0−6 μM). The insets show the changes in absorbance at 575 nm and emission intensity at 608 nm with increasing concentrations of Fe^{2+}.

additions of more Fe^{2+} did not result in any further spectral change. The titration profile (inset of Figure 8a) and the clear isosbestic point at 330 nm imply the single conversion of free **RuL** to form a Fe^{2+}−**RuL** complex. The Job plot shown in Figure S9 in the SI indicates that the Fe^{2+}−**RuL** complex has a stoichiometry of approximately 1:2. As shown in SI Figure S10, the luminescence intensity ratios of **RuL** in the presence and the absence of the metal cations were slightly affected by Na^+, Mg^{2+}, Ba^{2+}, Mn^{2+}, Zn^{2+}, Cd^{2+}, and Ag^+, were moderately quenched by Ni^{2+}, Hg^{2+}, and Fe^{3+}, and were severely quenched by Cu^{2+}, Fe^{2+}, and Co^{2+}. As shown in Figure 8b, the successive additions of Fe^{2+} into the Ru complex in the CH_3CN aqueous solution resulted in progressive quenching of the **RuL** emission to $I/I_0 = 0.06$ at saturation (0.5 equiv of Fe^{2+}). The selectivity of **RuL** toward Fe^{2+} in the CH_3CN aqueous solution was also evaluated. As shown in Figure S11 in the SI, Cu^{2+} elicited an almost full hypochromism at 575 nm of the Fe^{2+}−**RuL** complex; moreover, Na^+, Mg^{2+}, Ba^{2+}, Mn^{2+}, Fe^{3+}, Ni^{2+}, and Ag^+ only slightly affected the absorption at 575 nm, and Co^{2+}, Zn^{2+}, Cd^{2+}, and Hg^{2+} diminished the absorbances at 575 nm to different extents (the peaks were still clearly discerned). These results indicate the high selectivity of **RuL** toward Fe^{2+} over the other cations with the exception of Cu^{2+}. The above-mentioned UV−vis absorption and emission spectral behaviors of the Ru complex in the CH_3CN aqueous solution were similar to those (see SI Figures S12−S15) observed in neat CH_3CN. It should be highlighted that the coordination of the Zn^{2+}, Cd^{2+}, and Hg^{2+} ions with **RuL** in CH_3CN triggered slight emission enhancements ($I/I_0 < 1.2$) of **RuL** (Figure S12b in the SI); these changes are different from the spectral behaviors of **RuL** in an aqueous HEPES buffer/CH_3CN (71/1, v/v) solution.[11] The colorimetric limitation of detection (LOD) for Fe^{2+} in the CH_3CN aqueous solution was determined to be $\sim 4.58 \times 10^{-8}$ M (3σ/slope),[1h] which is slightly higher than the LOD value of $\sim 4.46 \times 10^{-8}$ M determined in neat CH_3CN. This finding indicates that **RuL** acted as a highly sensitive and selective colorimetric chemosensor toward Fe^{2+} in a CH_3CN−H_2O solution with a water content of up to at least 96.4% by volume. Thus, **RuL** has an advantage over the pure organic ligand of Htppip, which could tolerate a water content of less than 40% by volume.

Theoretical Insights into the Ion-Binding Modes of [Ru(bpy)$_2$(Htppip)]$^{2+}$. To obtain in-depth insights into the sensing mechanism of **RuL**, we performed the DFT calculations on **1**−**4** (see Scheme 2 and the corresponding atom-labeling scheme). The optimized structures of **1**−**4** are illustrated in SI Figure S16, and the main optimized structural parameters of **1**−**4** are summarized in SI Table S1. The optimized bond lengths of Ru−N and Fe−N in **1**−**4** are in reasonable agreement with the corresponding experimental values of analogous complexes.[1k,25] It should be noted that the imidazole N7−H bond length of **1** is 1.011 Å, which is much shorter than the length of the N7−H bond of **2** containing bound OAc^- (1.782 Å). This result shows that the H on the imidazole N7−H in **2** was transferred from the imidazolyl group of Htppip to OAc^-. The imidazole N7−H bond length in **3** is 1.066 Å and is a little longer than that in **1**, which supports the occurrence of a hydrogen-bond interaction between the N7−H of the imidazole and the O1 atom of $H_2PO_4^-$. The N7−C1−C2−C3 dihedral angles of **1**, **2**, and **3** are 5.41, −21.06, and 2.16°, respectively, and the C4−C5−C6−C7 dihedral angles of **1**, **2**, and **3** are −33.30, −35.83, and −32.43°, respectively. These results show that the phenyl and imidazole moieties are more coplanar in **3** than in **1**, which might explain the luminescence enhancement of [**Ru(bpy)$_2$(Htppip)**]$^{2+}$ that is observed upon binding to $H_2PO_4^-$. However, the N7−C1−C2−C3 dihedral angle of **2** is −21.06°, which indicates that the phenyl ring twisted upon binding to CH_3COO^-. It is noteworthy that there are one potential hydrogen bond of C3−H···O2 with bond lengths of 3.31 Å in **2** and two potential hydrogen bonds of C3−H···O1 and C8−H···O2 with bond lengths of 3.279 and 2.940 Å, respectively, in **3**. The fact that the bond length of C8−H···O2 in **3** is much shorter than that of C3−H···O1 in **3** is suggestive of the preferable formation of the latter one hydrogen bond in **3**. These hydrogen bond-forming evidence are in consistent with the proton NMR experimental observations.

The frontier molecular orbital compositions (population analysis using the self-consistent field density) of **1**−**4** are shown in Tables S2−S5 and Figure S17 in the SI. The calculated results show that the LUMO of **1** is dominantly contributed by bpy (92% π^*(bpy)) and is slightly affected by the additions of CH_3COO^- and $H_2PO_4^-$. The HOMOs of **1**−**3** dominantly localize on the Htppip ligand (99%) and the appreciable metal contributions (79% for **1**, 82% for **2**, and 81% for **3**) have only been predicted at the lower level (HOMO-10 for **1**, HOMO-11 for **2**, and HOMO-12 for **3**). The redshift (Figures 2a and 3a) of the MLCT band upon the addition of the OAc^- or $H_2PO_4^-$ anion can be rationalized based on the decreases in the energy gap from 3.71 eV in **1** (HOMO-10 → LUMO) to 3.44 eV in **2** (HOMO-11 → LUMO) and 3.48 eV in **3** (HOMO-12 → LUMO). Upon Fe^{2+} coordination, the distinct electron density transfer from HOMO-8 of Fe^{2+} to the LUMO of Htppip can be found (Figure S18 in the SI), implying that the MLCT process occurred in the [**Ru(bpy)$_2$(Htppip)**]$^{2+}$/Fe^{2+} complex.

CONCLUSIONS

In conclusion, we have shown that a Ru(II) polypyridyl complex with a terpyridine/phenylimidazo[4,5-*f*]-phenanthroline hybrid, which is denoted **RuL**, functions as an effective long wavelength emissive turn on luminescence sensor for $H_2PO_4^-$. This sensor is highly selective due to the turn off quenching type of response for F^- and OAc^- in both neat CH_3CN and CH_3CN/H_2O (50:1 v/v). The specific $H_2PO_4^-$ sensing was evidenced to be operative via intermolecular N−H···O hydrogen bonding between the O of $H_2PO_4^-$ and the imidazole NH of **RuL**, and O−H···N hydrogen bonding or

dx.doi.org/10.1021/ic301555r | Inorg. Chem. 2013, 52, 2306−2316

Scheme 2. Structural Schematic Diagram of the Complex Cations 1−4 with Numbers 1−8 Representing the Carbon Numbering Scheme for Optimized Structures by DFT Calculations

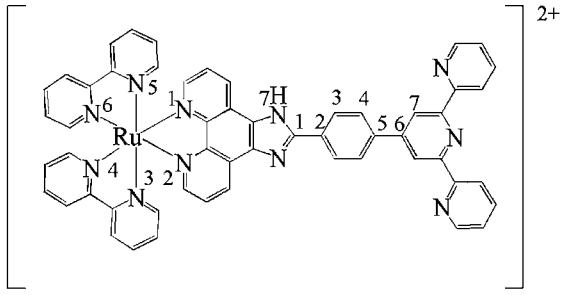

$[Ru(bpy)_2(Htppip)]^{2+}$ (**1**)

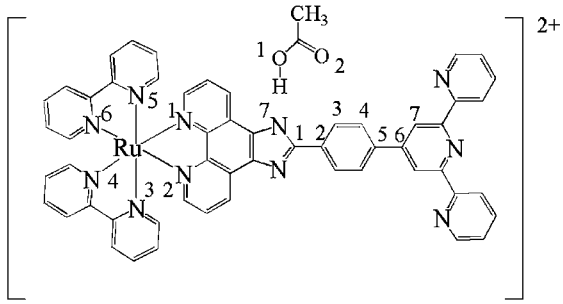

$[Ru(bpy)_2(Htppip)]^{2+}\cdot OAc^-$ (**2**)

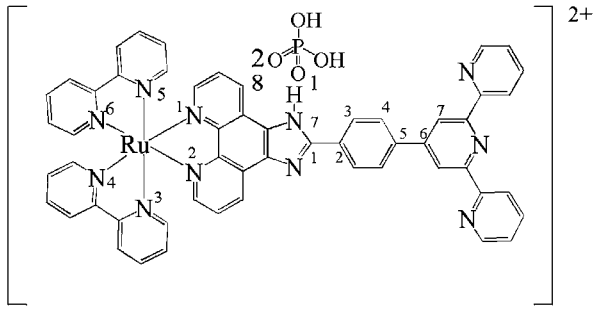

$[Ru(bpy)_2(Htppip)]^{2+}\cdot H_2PO_4^-$ (**3**)

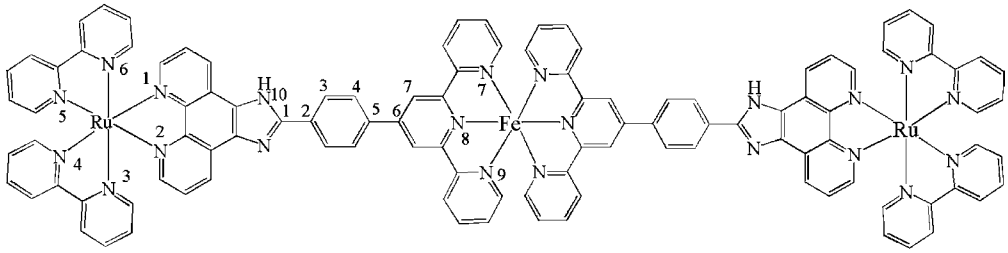

$Fe(II)\cdot\{[Ru(bpy)_2(Htppip)]^{2+}\}_2$ (**4**)

proton transfer between the OH of $H_2PO_4^-$ and the distal pyridine N of the terpyridine moiety on **RuL**. This mechanism is in contrast to the imidazole deprotonation mechanism that is observed in the interaction of **RuL** with F^- and OAc^- because $H_2PO_4^-$ -induced a much weaker **RuL** absorption at 368 nm than OH^-, F^-, and OAc^-. In addition, $H_2PO_4^-$ induced an enhanced emission compared with OH^-, F^-, and OAc^-, which quenched the emissions. **RuL** also acted as a highly selective colorimetric sensor for Fe^{2+} in both CH_3CN and aqueous HEPES buffer/CH_3CN solutions, which was evidenced through a color change from pale yellow to light red-purple to the naked eye. Thus, the simultaneous appending of

dx.doi.org/10.1021/ic301555r | Inorg. Chem. 2013, 52, 2306−2316

imidazole and free terpyridyl moieties in **RuL** plays a key role in the $H_2PO_4^-$ and Fe^{2+} sensing/recognition dual functions.

■ ASSOCIATED CONTENT

Supporting Information

Synthesis and characterization data, COSY spectrum of **RuL**, main geometry parameters of optimized structures, the effects of single additions of the anions and cations, and successive additions of Fe^{2+}, F^-, and OH^- on the UV−vis absorption and emission spectra, and emission intensity ratio of the Ru complex in CH_3CN as well as the solution color changes induced by single addition of anions, and Jobs plots for **RuL** with F^-, OAc^-, $H_2PO_4^-$, and Fe^{2+}. This material is available free of charge via the Internet at http://pubs.acs.org.

■ AUTHOR INFORMATION

Corresponding Author

*Author to whom all correspondence should be addressed. E-mail: kzwang@bnu.edu.cn. Fax: (+86-10-62200567). Tel: (+86-10-62205476).

Notes

The authors declare no competing financial interest.

■ ACKNOWLEDGMENTS

The authors thank the National Natural Science Foundation (21171022, 20971016, and 90922004) and Analytical and Measurements Fund of Beijing Normal University for financial supports.

■ REFERENCES

(1) (a) Schraderr, T.; Hamilton, A. D. *Functional Synthetic Receptors*; Wiley-VCH: Weinheim, Germany, 2005. (b) Caltagirone, C.; Gale, P. A. *Chem. Soc. Rev.* **2009**, *38*, 520. (c) Gale, P. A.; Garcia-Garrido, S. E.; Garric, J. *Chem. Soc. Rev.* **2008**, *37*, 151. (d) Du, J.; Hu, M.; Fan, J.; Peng, X. *Chem. Soc. Rev.* **2012**, *41*, 4511. (e) Wintergerst, M. P.; Levitskaia, T. G.; Moyer, B. A.; Sessler, J. L.; Delmau, L. H. *J. Am. Chem. Soc.* **2008**, *130*, 4129. (f) Yang, Z.; Yan, C.; Chen, Y.; Zhu, C.; Zhang, C.; Dong, X.; Yang, W.; Guo, Z.; Lu, Y.; He, W. *Dalton Trans.* **2011**, *40*, 2173. (g) Ahmed, N.; Geronimo, I.; Hwang, I. C.; Singh, N. J.; Kim, K. S. *Chem.—Eur. J.* **2011**, *17*, 8542. (h) Alfonso, M.; Espinosa, A.; Tárraga, A.; Molina, P. *Org. Lett.* **2011**, *13*, 2078. (i) Bhaumik, C.; Das, S.; Maity, D.; Baitalik, S. *Dalton Trans.* **2011**, *40*, 11795. (j) Zheng, Z. B.; Duan, Z. M.; Zhang, J. M.; Wang, K. Z. *Sensors Actuators B* **2012**, *169*, 312.

(2) (a) Fausto da Silva, J. J. R.; R. Williams, J. P. *The Biological Chemistry of the Elements*; Oxford University: New York, 1992. (b) Xu, Z.; Yoon, J.; Spring, D. R. *Chem. Soc. Rev.* **2010**, *39*, 1996.

(3) Scenger, W. *Principles of Nucleic Acid Structure*; Springer: New York, 1998.

(4) (a) Li, A. F.; Wang, J. H.; Wang, F.; Jiang, Y. B. *Chem. Soc. Rev.* **2010**, *39*, 3729. (b) Das, S.; Saha, D.; Bhaumik, C.; Duttab, S.; Baitalik, S. *Dalton Trans.* **2010**, *39*, 4162. (c) Chauhan, S. M. S.; Bisht, T.; Garg, B. *Tetrahedron Lett.* **2008**, *49*, 6646. (d) Kima, S. H.; Hwang, I. J.; Gwon, S. Y.; Burkinshawc, S. M.; Son, Y. A. *Dyes Pigm.* **2011**, *88*, 84.

(5) (a) Lee, H. N.; Swamy, K. M. K.; Kim, S. K.; Kwon, J.-Y.; Kim, Y.; Kim, S.-J.; Yoon, Y. J.; Yoon, J. *Org. Lett.* **2007**, *9*, 243. (b) Veale, E. B.; Gunnlaugsson, T. *J. Org. Chem.* **2008**, *73*, 8073. (c) Sessler, J. L.; Camiolo, S.; Gale, P. A. *Coord. Chem. Rev.* **2003**, *240*, 17. (d) Chang, K. J.; Moon, D.; Lah, M. S.; Jeong, K. S. *Angew. Chem., Int. Ed.* **2005**, *44*, 7926. (e) Makuc, D.; Lenarcic, M.; Bates, G. W.; Gale, P. A.; Plavec, J. *Org. Biomol. Chem.* **2009**, *7*, 3507. (f) Anzenbacher, P.; Nishiyabu, R.; Palacios, M. A. *Coord. Chem. Rev.* **2006**, *250*, 2929. (g) Aldakov, D.; Anzenbacher, P. *J. Am. Chem. Soc.* **2004**, *126*, 4752. (h) Moragues, M. E.; Martínez-Máñez, R.; Sancenón, F. *Chem. Soc. Rev.* **2011**, *40*, 2593. (i) Wenzel, M.; Hiscock, J. R.; Gale, P. A. *Chem. Soc. Rev.* **2012**, *41*, 480.

(6) (a) Tulyakova, E.; Delbaere, S.; Fedorov, Y.; Jonusauskas, G.; Moiseeva, A.; Fedorova, O. *Chem.—Eur. J.* **2011**, *17*, 10752. (b) Nolan, E. M.; Lippard, S. J. *Chem. Rev.* **2008**, *108*, 3443. (c) Huang, W.; Wu, D. Y.; Wu, G. H.; Wang, Z. Q. *Dalton Trans.* **2012**, *41*, 2620. (d) He, X.; Yam, V. W. W. *Inorg. Chem.* **2010**, *49*, 2273.

(7) (a) Bandyopadhyay, P.; Ghosh, A. K. *J. Phys. Chem. B* **2009**, *113*, 13462. (b) You, Y.; Lee, S.; Kim, T.; Ohkubo, K.; Chae, W. Si.; Fukuzumi, S.; Jhon, G. J.; Nam, W.; Lippard, S. J. *J. Am. Chem. Soc.* **2011**, *133*, 18328. (c) Zhao, Q.; Li, F.; Huang, C. *Chem. Soc. Rev.* **2010**, *39*, 3007. (d) Araya, J. C.; Gajardo, J.; Moya, S. A.; Aguirre, P.; Toupet, L.; Williams, J. A. G.; Escadeillas, M.; Le Bozec, H.; Guerchais, V. *New J. Chem.* **2010**, *34*, 21. (e) Stepanov, A. S.; Yanilkin, V. V.; Mustafina, A. R.; Burilov, V. A.; Solovieva, S. S.; Antipin, I.; Konovalov, A. I. *Electrochem. Commun.* **2010**, *12*, 703. (f) Wade, C. R.; Ke, I. S.; Gabbaï, F. P. *Angew. Chem., Int. Ed.* **2012**, *51*, 478. (g) Happ, B.; Winter, A.; Hager, M. D.; Schubert, U. S. *Chem. Soc. Rev.* **2012**, *41*, 2222.

(8) (a) Fan, S. H.; Zhang, A. G.; Ju, C. C.; Gao, L. H.; Wang, K. Z. *Inorg. Chem.* **2010**, *49*, 3752. (b) Fan, S. H.; Li, Q.; Wang, K. Z. *Inorg. Chim. Acta* **2009**, *362*, 5155. (c) Zhao, X. L.; Han, M. J.; Zhang, A. G.; Wang, K. Z. *J Inorg. Biochem.* **2012**, *107*, 104. (d) Ju, C. C.; Zhang, A. G.; Yuan, C. L.; Zhao, X. L.; Wang, K. Z. *J. Inorg. Biochem.* **2011**, *105*, 435. (e) Luo, H.; Wang, Z. P.; Zhang, A. G.; Wang, K. Z. *Aus. J. Chem* **2011**, *64*, 206. (f) Yang, H. X.; Liu, Y. J.; Zhao, L.; Wang, K. Z. *Spectrochim. Acta A* **2010**, *76*, 146.

(9) (a) Kitchen, J. A.; Boyle, E. M.; Gunnlaugsson, T. *Inorg. Chim. Acta* **2012**, *381*, 236. (b) Sam, N. A.; Alexander, V. *Dalton Trans.* **2011**, *40*, 8630. (c) Li, Z. Z.; Liang, Z. H.; Huang, H. L.; Liu., Y. J. *J. Mol. Struct.* **2011**, *1001*, 36.

(10) (a) Kim, J. S.; Quang, D. T. *Chem. Rev.* **2007**, *107*, 3780. (b) Sessler, J. L.; Kim, S. K.; Gross, D. E.; Lee, C.-H.; Kim, J. S.; Lynch, V. M. *J. Am. Chem. Soc.* **2008**, *130*, 13162. (c) Buccella, D.; Horowitz, J. A.; Lippard, S. J. *J. Am. Chem. Soc.* **2011**, *133*, 4101. (d) McQuade, L. E.; Lippard, S. J. *Inorg. Chem.* **2010**, *49*, 7464. (e) You, Y.; Tomat, E.; Hwang, K.; Atanasijevic, T.; Nam, W.; Jasanoff, A. P.; Lippard, S. J. *Chem. Commun.* **2010**, *46*, 4139. (f) Du, P.; Lippard, S. J. *Inorg. Chem.* **2010**, *49*, 10753.

(11) (a) Hofmeier, H.; Schubert, U. S. *Chem. Soc. Rev.* **2004**, *33*, 373. (b) Hayami, S.; Komatsu, Y.; Shimizu, T.; Kamihata, H.; Lee, Y. H. *Coord. Chem. Rev.* **2011**, *255*, 1981. (c) Cui, Y.; Chen, Q.; Zhang, D. D.; Cao, J.; Han, B. H. *J. Polym. Sci., Part A: Polym. Chem.* **2010**, *48*, 1310. (d) Meier, M. A. R.; Schubert, U. S. *Chem. Commun.* **2005**, 4610. (e) Liang, Z. Q.; Wang, C. X.; Yang, J. X.; Gao, H. W.; Tian, Y. P.; Tao, X. T.; Jiang, M. H. *New J. Chem.* **2007**, *31*, 906. (f) Kimura, M.; Horai, T.; Hanabusa, K.; Shirai, H. *Adv. Mater.* **1998**, *10*, 459.

(12) Sullivan, B. P.; Meyer, T. J. *Inorg. Chem.* **1978**, *17*, 3334.

(13) Bodige, S.; MacDonnell, F. M. *Tetrahedron Lett.* **1997**, *38*, 8159.

(14) Duprez, V.; Krebs, F. C. *Tetrahedron Lett.* **2006**, *47*, 3785.

(15) (a) Abou-Zied, O. K. *J. Phys. Chem. B* **2007**, *111*, 9879. (b) Wu, Y. K.; Peng, X. J.; Fan, J. L.; Gao, S.; Tian, M. Z.; Zhao, J. Z.; Sun, S. G. *J. Org. Chem.* **2007**, *72*, 62.

(16) (a) Zhao, Y.; Truhlar, D. G. *Theor. Chem. Acc.* **2008**, *120*, 215. (b) Zhao, Y.; Truhlar, D. G. *Acc. Chem. Res.* **2008**, *41*, 157.

(17) Frisch, M. J.; Trucks, G. W.; Schlegel, H. B.; Scuseria, G. E.; Robb, M. A.; Cheeseman, J. R.; Zakrzewski, V. G.; Montgomery, J. A., Jr.; Stratmann, R. E.; Burant, J. C.; Dapprich, S.; Millam, J. M.; Daniels, A. D.; Kudin, K. N.; Strain, M. C.; Farkas, O.; Tomasi, J.; Barone, V.; Cossi, M.; Cammi, R.; Mennucci, B.; Pomelli, C.; Adamo, C.; Clifford, S.; Ochterski, J.; Petersson, G. A.; Ayala, P. Y.; Cui, Q.; Morokuma, K.; Malick, D. K.; Rabuck, A. D.; Raghavachari, K.; Foresman, J. B.; Cioslowski, J.; Ortiz, J. V.; Stefanov, B. B.; Liu, G.; Liashenko, A.; Piskorz, P.; Komaromi, I.; Gomperts, R.; Martin, R. L.; Fox, D. J.; Keith, T.; Al-Laham, M. A.; Peng, C. Y.; Nanayakkara, A.; Gonzalez, C.; Challacombe, M.; Gill, P. M. W.; Johnson, B. G.; Chen, W.; Wong, M. W.; Andres, J. L.; Head-Gordon, M.; Replogle, E. S.; Pople, J. A. *Gaussian 09*, Revision A.02; Gaussian Inc.: Wallingford CT, 2009.

(18) (a) Dunning Jr., T. H.; Hay, P. J. *Modern Theoretical Chemistry*, 3rd ed.; Schaefer, H. F., Ed.; Plenum: New York, 1976; pp 1−28. (b) Hay, P. J.; Wadt, W. R. *J. Chem. Phys.* **1985**, *82*, 299.
(19) During our preparation of this manuscript, syntheses of the complex were reported: (a) Hamelin, O.; Guillo, P.; Loiseau, F.; Boissonnet, M. F.; Ménage, S. *Inorg. Chem.* **2011**, *50*, 7952. (b) Herrero, C.; Quaranta, A.; Protti, S.; Leibl, W.; Rutherford, A. W.; Fallahpour, D. R.; Charlot, M. F.; Aukauloo, A. *Chem. Asian J.* **2011**, *6*, 1335.
(20) Ghosh, A.; Ganguly, B.; Das, A. *Inorg. Chem.* **2007**, *46*, 9912.
(21) (a) Cui, Y.; Mo, H. J.; Chen, J. C.; Niu, Y. L.; Zhong, Y. R.; Zheng, K. C.; Ye, B. H. *Inorg. Chem.* **2007**, *46*, 6427. (b) Shang, X. F.; Li, X. J.; Xi, N. K.; Zhai, Y. T.; Zhang, J. L.; Xu, X. F. *Sensors Actuators B* **2011**, *160*, 1112. (c) Saha, D.; Das, S.; Bhaumik, C.; Dutta, S.; Baitalik, S. *Inorg. Chem.* **2010**, *49*, 2334. (d) Chen, H. M.; Li, J. W.; Lin, H.; Cai, Z. S.; Lin, H. K. *Supramol. Chem.* **2009**, *21*, 401. (e) Lazarides, T.; Miller, T. A.; Jeffery, J. C.; Ronson, T. K.; Adams, H.; Ward, M. D. *Dalton Trans.* **2005**, 528. (f) Bhaumik, C.; Saha, D.; Das, S.; Baitalik, S. *Inorg. Chem.* **2011**, *50*, 12586. (g) Mo, H. J.; Niu, Y. L.; Zhang, M.; Qiao, Z. P.; Ye, B. H. *Dalton Trans.* **2011**, *40*, 8218.
(22) (a) Szemes, F.; Hesek, D.; Chen, Z.; Dent, S. W.; M. Drew, G. B.; Goulden, A. J.; Graydon, A. R.; Grieve, A.; Mortimer, R. J.; Wear, T.; Weightman, J. S.; Beer, P. D. *Inorg. Chem.* **1996**, *35*, 5868. (b) Saha, D.; Das, S.; Mardanya, S.; Baitalik, S. *Dalton Trans.* **2012**, *41*, 8886.
(23) Liu, Y.; Li, Z.; Zhang, H. Y.; Wang, H.; Li, C. J. *Supramol. Chem.* **2008**, *20*, 419.
(24) (a) Du, K. J.; Wang, J. Q.; Kou, J. F.; Li, G. Y.; Wang, L. L.; Chao, H.; Ji, L. N. *Eur. J. Med. Chem.* **2011**, *46*, 1056. (b) Quaranta, A.; Lachaud, F.; Herrero, C.; Guillot, R.; Charlot, M. F.; Leibl, W.; Aukauloo, A. *Chem.—Eur. J.* **2007**, *13*, 8201.
(25) (a) Lide, D. R. *Handbook of Chemistry and Physics*, 90th ed.; CRC Press: Boca Raton, FL, 2009. (b) Mo, H. J.; Wu, J. J.; Qiao, Z. P.; Ye, B. H. *Dalton Trans.* **2012**, *41*, 7026. (c) Gao, J.; Wang, Z. P.; Yuana, C. L.; Jia, H. S.; Wang, K. Z. *Spectrochim. Acta A* **2011**, *79*, 1815. (d) El-Gahami, M. A.; Ibrahim, S. A.; Fouad, D. M.; Hammam, A. M. *J. Chem. Eng. Data* **2003**, *48*, 293.